# Core x-ray spectra in semiconductors and the Mahan-Nozieres-De Dominicis model

Peteris Livins
*Department of Physics and Astronomy, Western Washington University, Bellingham, Washington 98225*
(Received 16 October 1997; revised manuscript received 17 June 1998)

The Mahan-Nozières-De Dominicis (MND) model of core x-ray spectra is examined for semiconductors. Due to the finite band gap, the Anderson orthogonality does not occur, and thus spectra near the band edge can be calculated without the shakeup contribution. For semiconductors, and not only for metals, we investigate whether the remaining many-particle dynamic exchange effect of the MND model, or so-called replacement, can significantly alter x-ray spectral shapes near the band edge from those obtained from a straightforward final-state rule. For both emission and absorption, in the absence of shakeup, an exact formulation suitable for materials with band structure is discussed. A numerical model for a semiconductor with a 1-eV band gap demonstrates the band-edge modifications, and shows a 50% effect at the band edge, indicating that this dynamic exchange effect can be significant and should be considered in any specific emission or absorption calculation for a semiconductor. Although the ineffectiveness of the orthogonality theorem in semiconductors is emphasized, a suppression near the band edge also remains a possibility. Included is a discussion on the breakdown of the final-state rule. In addition, connection is made to the determinantal approach of Ohtaka and Tanabe. [S0163-1829(98)01040-6]

## I. INTRODUCTION

Since the recognition of the edge singularity in the x-ray spectra of metals,[1,2] and the Anderson orthogonality theorem,[3] much effort has been extended to obtaining improved theoretical descriptions of core spectroscopies of metals within the Mahan-Nozières–DeDominicis (MND) model.[4,5] This model embodies the most significant many-body effects in core-spectroscopies. Its most curious prediction for metals is that in certain cases one expects an integrable divergence at the emission or absorption edges. Another surprising result is the so-called final-state rule, which specifies what effective single-particle electron states, used in a single-particle calculation, best reflect the many-particle spectra. Disentangling these many-particle spectral modifications is of course important to the experimental determination of the independent electron structure. Here we will address the modifications occurring in the soft x-ray spectra of semiconductors. In particular, there is the question of whether the edge enhancement occurring in metals is significant in nonmetals.

For metals, Nozières and DeDominicis (ND) [Ref. 2] use a contact potential and calculate the appropriate response function in obtaining the spectral asymptotic limit. Their solution quantitatively predicts a power-law behavior $|\omega-\omega_0|^{\alpha}$ in terms of the photon energy $\omega$, measured from the absorption or emission threshold $\omega_0$. The exponent is given by

$$\alpha=-2[\delta_l/\pi]+\sum_{l'} 2(2l'+1)[\delta_{l'}/\pi]^2. \qquad (1)$$

The partial-wave phase shifts $\delta_{l'}$ for each angular momentum component $l'$, evaluated at the Fermi energy, describe the core-hole potential. The component $l$ specifies the angular momentum for the valence electron that is active in the transition to or from the core state, and that thus satisfies the dipole selection rule with that core state. The ND solution incorporates two competing effects in the edge region. The first term in the above exponent is the diverging contribution discovered by Mahan, the other gives a suppression of the edge spectra, related to the Anderson orthogonality. Features away from the edge region were later noted to follow a final-state rule.[6–9]

Alternatively, the MND model is equivalent[10,11] to calculating the x-ray spectra using Slater determinantal many-particle states constructed from self-consistent initial and final single-particle electron states. Thus two orthonormal sets of single-particle states are noted, $|\psi_i\rangle$ for the undistorted states, $|\phi_i\rangle$ for the distorted states in the presence of the core-hole. The transition rate is then formulated through the Fermi golden rule in terms of the many-particle transition matrix elements. In this approach, one makes distinction between a primary transition and a shakeup transition. We define a primary transition as one resulting in the transfer of just a single electron between a valence and a core state. The shakeup transitions instead appear as primary transitions accompanied by one or more valence electrons simultaneously promoted to unoccupied valence states. The determinantal approach emphasizes that the divergent behavior of the MND edge feature is a consequence of a dynamic exchange process during the x-ray transition. Friedel[10] pointed out that the divergence occurs due to the contribution of what he named ''replacement terms,'' which arise in the transition element due to the antisymmetrization. We distinguish this dynamic exchange feature from the exchange-correlation potentials used to calculate self-consistent independent single-particle electron states.

The most complete theoretical solution to the MND problem to date has been obtained by Ohtaka and Tanabe (OT).[5,12] Unlike the ND solution, their method is based on determinants, where all shakeup contributions have been summed. For a simple contact potential, the OT solution obtains analytic results throughout the complete spectral range,

 

not just in the edge region. In the determinantal approach for metals, the focus of summing all shakeup contributions can be traced to the Anderson orthogonality theorem for metals. By direct evaluation,[3] Anderson has shown that the overlap $\rho=\langle\Psi_0|\Phi_0\rangle$ between the ground states of two many-particle states, $|\Psi_0\rangle$ and $|\Phi_0\rangle$, constructed from Slater determinants of plane and scattered single-electron wave functions, vanishes as $N$ increases. The Anderson theorem implies that for $N$ particles, any one particular transition, primary or shakeup, occurs with vanishing probability as $N$ increases to infinity. Hence, to obtain a finite analytic result for $10^{23}$ electrons, all transitions to infinite shakeup order are required. We see that in metals the contribution purely from primary transitions alone are then overwhelmed by the shakeup contribution. However, the information in the primary spectrum is not lost, it is convoluted in a complicated manner with the shakeup contributions. The total result is, from what one may expect from the primary transitions alone, that the shape of the resulting total spectrum is only largely modified from the primary spectrum near the edge regions, and also in the low-energy tail for emission. Except in the case of the edge suppression in metals, the spectrum obtained from the primary transitions alone does include the dominant many-particle effect. The Mahan edge singularity, as also the final-state rule, are in fact identified with the primary spectrum. It is the complicated convoluting of the shake-up processes that may or may not suppress the edge singularity in metals, as the ND formula, Eq. (1), indicates.

The Anderson orthogonality is important in metals. However, this report will instead primarily concern itself with the influence of the many-particle effects in the spectra of filled band materials with small to moderate band gaps, such as semiconductors. In materials with a finite band gap, the orthogonality theorem will not be effective, and hence the spectra can be to a large degree described by the primary transitions alone. To recognize this, we need only note experiment. If the orthogonality were to apply to filled band materials, then an additional spectral gap, beyond the energy gap, would appear between emission and absorption in the same material. For if the orthogonality were to block a primary transition from the top of a filled band in emission, then only shakeup transitions would allow for the largest emission transition energy, diminishing the photon energy by at least the band-gap energy required to simultaneously promote the shakeup electron. On the other hand, in absorption, the least energetic threshold photon would not only promote an electron from the core to the lowest unoccupied state, but also an electron across the gap. This would increase the required photon energy by at least a band-gap energy. Thus an additional spectral gap of at least twice the energy gap would occur between the emission spectra and absorption spectra. This is never observed. In both emission or absorption, the overall relaxation energy shift contributes to the photon energy in the same way, and would not have an effect with regard to any spectral energy gap. Thus near the band edge in the spectra of semiconductors, the Anderson suppression does not enter, only the Mahan divergent effect does, which could then provide a remnant of the edge singularity found in metals.

There is evidence[13] that shakeup in semiconductors is certainly not negligible, but when it is significant, it does not contribute at energies near the boundary between occupied and unoccupied states. This is in contrast to the case of metals. To understand this, we focus on the case of emission. As mentioned, the shape of the spectral contribution from the shakeup can be viewed approximately as a convolution of the primary transition spectrum with a function that characterizes the energy dependence of the single-particle shakeup probabilities. The shakeup energy is the energy gain an electron obtains in jumping to an unoccupied state. The probability amplitudes for such shakeup processes are related to the single-particle overlaps $S_{ij}\equiv\langle\psi_j|\phi_i\rangle$, where state $i$ and $j$ lie on opposite sides of the Fermi level. In metals, the function that determines the shakeup probability energy dependence is characterized by a relatively narrow function of energy located near zero shakeup energy. This is because the shakeup probability to unoccupied single-particle states decays with energy measured from occupied states. Since a metal lacks a band gap, the most significant shakeup energies are the closest, small energies. In metals, covoluting the primary spectrum with this narrow function produces little change from the primary spectrum, except at the Fermi edge, and also in the formation of a low-energy tail for emission. In contrast, for filled band materials, the appropriate characteristic function to convolute with is offset from zero by at least the energy gap. Its centroid is further offset because the density of unoccupied states right above the gap is small and only then increases. Finally, the centroid of the primary spectrum in semiconductors is largest not near the unoccupied states, but lower in energy. Thus the approximate convolution leading to the resulting shakeup contribution is expected to peak at the lower energy end of the emission spectrum. Therefore, the shakeup contribution remains insignificant for much of the high-energy end of the emission band. It is of course rigorously zero within a band gap from the band edge.

It should be noted that near the edge emission in a semiconductor, unlike in metals, the single-particle density of states for a nonmetal approaches zero. Contrary to metals then, any many-body enhancement of the spectra, giving deviation from what one would expect from the final-state rule, is not strikingly apparent from experiment without a detailed comparison to calculated final-state spectra. Likewise, in absorption, the distinction between a many-particle dynamic exchange enhancement and an excitonic enhancement due simply to a final-state attractive potential, also requires a closer examination. Here, we address the question of any such band-edge modifications in nonmetals, and develop a straightforward formalism for their understanding within the framework of ordinary band-structure calculations.

## II. PARTIALLY INVERTED INITIAL STATES

Having recognized that the primary spectrum can be expected to dominate in the x-ray spectra of semiconductors, we omit in the following the shakeup contribution, and only consider the primary spectrum. This, however, will retain the major dynamic exchange effect of the MND model. It will become apparent that the spectral behavior discussed here, whether for emission or absorption, will be better understood through an emission process. Thus, we shall remain focused on the emission problem, although much of the discussion will also be relevant to absorption. The extensions to absorption are discussed in Sec. IV.

In the determinantal description of the emission process one considers transition matrix elements $T_{fi}$ between the initial and final many-particle states with energies $E_i$ and $E_f$, respectively. By the Fermi golden rule, the transition rate as a function of photon energy is proportional to a function $I(\omega)$ given by

$$I(\omega)=\sum_f |T_{fi}|^2 \delta(\omega+E_i-E_f). \tag{2}$$

For x-ray photons, the slowly varying factor involving the photon frequency is here suppressed for the relatively narrow band energy range. Since we omit the shakeup contributions, the final many-particle states for emission are limited to those with a single vacant level somewhere within the ordinarily filled band. The many-particle transition matrix elements $T_{fi}$ will involve determinants of matrices composed of single-particle overlaps and single-particle transition matrix elements.[10] An exact simplified analysis occurs for each such many-particle matrix element when one employs the single-particle states[13] $|\overline{\phi}_n\rangle$ given by

$$|\overline{\phi}_n\rangle=\sum_{i=\mathrm{occ}} s_{ni}^{-1}|\phi_i\rangle, \tag{3}$$

where $s^{-1}$ is the inverse matrix for the occupied submatrix $s_{nm}=S_{nm}\equiv\langle\psi_m|\phi_n\rangle$ ($n,m$ occupied) of the full unitary matrix $S$. These partially inverted initial states, so called because they represent an incomplete transformation from initial distorted state $|\phi_n\rangle$ to final undistorted state $|\psi_n\rangle$, are orthogonal to all *occupied undistorted* states. Observe that the Kronecker delta

$$\delta_{ij}=\sum_{k=\mathrm{occ}} s_{ik}^{-1}s_{kj}=\langle\psi_j|\sum_{k=\mathrm{occ}} s_{ik}^{-1}|\phi_k\rangle=\langle\psi_j|\overline{\phi}_i\rangle, \tag{4}$$

for $i$ and $j$ occupied. However, the states $|\overline{\phi}_n\rangle$ are not normalized.

To verify the simplification introduced by such single-particle states, we consider the many-particle transition matrix element $T_n=\langle\Psi(n)|\Sigma_m t_m|\Phi_0\rangle$, where $t_m$ represents the optical transition operator for particle $m$. For instance, the dipole operator. Here $\Psi(n)$ is the $N$ particle state with a valence hole in state $n$, but with the core state $|\mathrm{core}\rangle$ filled. Implicit within the MND model is a ''frozen core'' approximation, in which the overlaps $\langle\mathrm{core}|\psi\rangle$ and $\langle\mathrm{core}|\phi\rangle$ are considered negligible for both orthonormal sets. Hence, the relevant many-particle transition matrix element $T_n$ reduces to calculating the determinant of a single matrix $M_n$ constructed from elements which are single-particle overlaps $S_{nm}$ and single-particle transition matrix elements $\langle\mathrm{core}|t|\phi_n\rangle\equiv\langle\tilde{c}|\phi_n\rangle$. Following Friedel,[10] the matrix $M_n$ has the form

$$M_n=\begin{pmatrix} \langle\psi_1|\phi_1\rangle & \cdots & \langle\psi_1|\phi_n\rangle & \cdots & \langle\psi_1|\phi_N\rangle \\ \langle\psi_2|\phi_1\rangle & \cdots & \cdots & \cdots & \langle\psi_2|\phi_N\rangle \\ \vdots & \vdots & \vdots & \vdots & \vdots \\ \langle\tilde{c}|\phi_1\rangle & \cdots & \langle\tilde{c}|\phi_n\rangle & \cdots & \langle\tilde{c}|\phi_N\rangle \\ \vdots & \vdots & \vdots & \vdots & \vdots \\ \langle\psi_N|\phi_1\rangle & \cdots & \langle\psi_N|\phi_n\rangle & \cdots & \langle\psi_N|\phi_N\rangle \end{pmatrix}, \tag{5}$$

where the single-particle transition matrix elements replace the $n$th row.

In considering the determinant of this matrix, we note that $\det M_n=\det(M_n^T)=\det(s)\det(s^{-1}M_n^T)$. Furthermore, due to the orthonormality condition of Eq. (4), the matrix $s^{-1}M_n^T$ has off-diagonal elements that are zero, except for column $n$. For all elements with $k\neq n$, $(s^{-1}M_n^T)_{ik}=\Sigma_{j=\mathrm{occ}}s_{ij}^{-1}\langle\psi_k|\phi_j\rangle=\Sigma_{j=\mathrm{occ}}\langle\psi_k|s_{ij}^{-1}|\phi_j\rangle=\langle\psi_k|\overline{\phi}_i\rangle$, while for the case $k=n$, $(s^{-1}M_n^T)_{in}=\Sigma_{j=\mathrm{occ}}\langle\tilde{c}|s_{ij}^{-1}|\phi_j\rangle=\langle\tilde{c}|\overline{\phi}_i\rangle$. Thus $s^{-1}M_n^T$ is similar to the matrix $M_n^T$, but where the elements have been constructed with all states $|\phi_i\rangle$ replaced by the transformed states $|\overline{\phi}_i\rangle$.

This last observation leads to a trivial evaluation of $\det(s^{-1}M_n^T)$, giving

$$T_n=\det(s)(-1)^{n+1}\langle\tilde{c}|\overline{\phi}_n\rangle\langle\psi_1|\overline{\phi}_1\rangle \times\langle\psi_2|\overline{\phi}_2\rangle\cdots(\mathrm{no}\langle\psi_n|\overline{\phi}_n\rangle)\cdots\langle\psi_N|\overline{\phi}_N\rangle. \tag{6}$$

It now appears that the passive electron overlap $\langle\psi_1|\overline{\phi}_1\rangle\langle\psi_2|\overline{\phi}_2\rangle\cdots(\mathrm{no}\langle\psi_n|\overline{\phi}_n\rangle)\cdots\langle\psi_N|\overline{\phi}_N\rangle$, with further $n$ dependence, remains. However, the mentioned orthonormality assures that in the diagonal product of Eq. (6), we have $\langle\psi_i|\overline{\phi}_i\rangle=1$, thus voiding any $n$-dependent passive overlap. For each case $n$, the transformation on the distorted states introduces the *common* factor $\det(s)=\langle\Psi_0|\Phi_0\rangle=\rho$, giving the simplified result

$$|T_n|^2=|\rho|^2|\langle\mathrm{core}|t|\overline{\phi}_n\rangle|^2. \tag{7}$$

As anticipated, the Anderson factor $|\rho|^2$ enters. This effective single-particle matrix element then provides the exact transition probability within the MND model when shakeup is negligible. It is such an analysis of emission, rather than absorption, that leads to the particularly simple result of Eq. (7), due to a common transformation factor. We distinguish here the orthogonalized final state (OFS) of Davis and Feldkamp,[14] which, however, does not give an exact effective state, particularly in the edge region. As a consequence, the OFS state predicts a logarithmic edge singularity in metals,[15] instead of a power law.

The final-state rule specifies that the best effective single-particle states to use in a one-particle description of emission or absorption are those appropriate to the final-state potentials. In emission this will imply the undistorted states $|\psi_n\rangle$. The partially inverted initial state, as defined by Eq. (3), provides a natural theoretical explanation.[13] The imposed orthogonalization exhibited by the state $|\overline{\phi}_i\rangle$ forces it to approach its corresponding undistorted state $|\psi_i\rangle$. This occurs most strongly to occupied states $i$ that are far in energy from unoccupied states. In these cases the components $S_{ij}$ to unoccupied states $j$ are relatively small, such that the distorted state $i$ can be effectively spanned by states within the subset of occupied undistorted states. This then allows for an approximate orthonormalization within all the undistorted states, and thus the transformed state must be very similar to its corresponding undistorted state. This orthonormalizing effect will slowly diminish as the energy of the state $i$ approaches unoccupied states. We show below, that slowly means approximately logarithmically with the energy difference to unoccupied states. This initial logarithmic depen-

dence eventually begins turning to a more rapid spectral enhancement upon nearing the edge region, even in semiconductors. Hence, the effect of replacement is responsible for both the final-state rule, as well as deviations from it, in the form of an edge enhancement.

### III. BAND-EDGE MODIFICATIONS

Further interpretation of the state $|\overline{\phi}_n\rangle$ is obtained when written in terms of the undistorted states $|\psi_j\rangle$. Expanding in the complete set $|\psi_j\rangle$, and invoking the resulting Kronecker delta, gives

$$|\overline{\phi}_n\rangle = \sum_{i=\mathrm{occ}} s_{ni}^{-1}\left( \sum_{j=\mathrm{occ}} S_{ij}|\psi_j\rangle + \sum_{j=\mathrm{unocc}} S_{ij}|\psi_j\rangle \right)$$

$$= |\psi_n\rangle + \sum_{i=\mathrm{occ}} s_{ni}^{-1} \sum_{j=\mathrm{unocc}} S_{ij}|\psi_j\rangle. \quad (8)$$

The first term conforms to the final-state rule, while the second term contains elements $S_{ij}$, which only couple between occupied states $i$ and unoccupied states $j$. Besides the constant factor $\rho$, it is now evident that deviation from independent electron behavior is reflected in the second term, which arises from both the effective interaction of the electron with the core hole and the requirements on particle exchange. The emission at the energy corresponding to a transition leaving a sole valence hole in the single-particle state $n$ will be determined by

$$|T_n|^2 = \rho^2 \left| \langle \tilde{c}|\psi_n\rangle + \sum_{i=\mathrm{occ}} s_{ni}^{-1} \sum_{j=\mathrm{unocc}} S_{ij}\langle \tilde{c}|\psi_j\rangle \right|^2. \quad (9)$$

In a metal where the ions are modeled with a uniform positive background, different angular momentum states are decoupled, and thus would make a separate contribution to $T_n$. Normalized delocalized undistorted states of the same angular momentum have dipole matrix elements with magnitudes that vary slowly with energy. Actual solids of course exhibit an energy-dependent hybridization of angular momentum states, and this will increase the energy variation of $\langle \tilde{c}|\psi_n\rangle$. However, it will help to elucidate Eq. (9) if we set the single-particle transition matrix elements $\langle \tilde{c}|\psi_n\rangle$ to the constant factor 1, and consider instead

$$|T_n|^2 = \rho^2 |1 + \sum_{i=\mathrm{occ}} s_{ni}^{-1} \sum_{j=\mathrm{unocc}} S_{ij}|^2 \equiv \Lambda_n. \quad (10)$$

The only loss of generality comes from the constant magnitude of $\langle \tilde{c}|\psi_n\rangle$, since we may always choose the state phases so that the transition matrix elements $\langle \tilde{c}|\psi_n\rangle$ are real and positive. We denote the second term in Eq. (10), which we call the mixing term, by

$$h_n = \sum_{i=\mathrm{occ}} s_{ni}^{-1} \sum_{j=\mathrm{unocc}} S_{ij} = \sum_{i=\mathrm{occ}} s_{ni}^{-1} g_i, \quad (11)$$

where $g_i = \Sigma_{j=\mathrm{unocc}} S_{ij}$.

The introduction of the core-hole potential produces an impurity scattering problem for the distorted wave functions. We write $H = H_0 + v_h$ and $H_0$ for the single-particle Hamiltonians that include and exclude the core-hole potential $v_h$, respectively. Then the distorted state $|\phi_i\rangle = \Sigma_{k=\mathrm{all}} S_{ik}|\psi_k\rangle$ satisfies

$$H|\phi_i\rangle = \tilde{\epsilon}_i|\phi_i\rangle, \quad (12)$$

and the undistorted states satisfy

$$H_0|\psi_i\rangle = \epsilon_i|\psi_i\rangle, \quad (13)$$

where $\epsilon_i$ and $\tilde{\epsilon}_i$ are the energies of the undistorted and distorted states, respectively. Substitution of the expanded distorted state into Eq. (12) leads to the standard eigenvalue problem. For each $j$,

$$\sum_{k=\mathrm{all}\neq j} v_{jk}S_{ik} + (v_{jj} + \epsilon_j)S_{ij} = \tilde{\epsilon}_i S_{ij}, \quad (14)$$

where $v_{jk} = \langle \psi_j|v_h|\psi_k\rangle$, which become uniquely specified with the above-mentioned phase restriction.

For a general understanding and illustration of the emergence of the edge singularity from Eq. (10), we deduce the behavior of the mixing term. For this purpose, first-order perturbation theory will suffice. The overlap elements are specified to first order by

$$S_{ij} \approx z_i \left( \delta_{ij} + \frac{v_{ji}}{(\epsilon_i - \epsilon_j)} \right). \quad (15)$$

The factor $z_i$ is the normalization factor for the distorted state $i$. It can always be chosen real and positive, and it then has a value that is ordinarily close to 1. For the present discussion, it is assumed that the single-particle matrix element $v_{ji}$ for the attractive potential is a negative constant $v = -|v|$. Consider the summation defining $g_i$. Since the energy of the unoccupied state $j$ is always greater than the energy of occupied state $i$, and $v$ is negative, $g_i$ is always positive. To discern how the factor $g_i$ behaves with the energy of state $i$, consider the integral approximation $\int_{\epsilon_g}^{C} S_{ij} n_0 d\epsilon_j$ to the defining sum for $g_i$, using a constant density of states $n_0$, and an integration cutoff $C \gg |\epsilon_i|$. Here $\epsilon_g$ is the energy gap between occupied and unoccupied states, thus the energy zero corresponds to the highest occupied state. Insertion of Eq. (15) shows that $g_i$ varies with $\epsilon_i$ typically like $z n_0 |v| \ln((C + |\epsilon_i|)/(|\epsilon_i| + \epsilon_g)) \approx z n_0 |v| [\ln(C) - \ln(|\epsilon_i| + \epsilon_g)]$, where the average value for $z_i$ is $z \approx 1$. Thus, $g_i$ varies *slowly* with energy $\epsilon_i$ until the edge region is approached, at which point, if $\epsilon_g$ is not finite, $g_i$ diverges logarithmically. Figure 1(a) gives an example of $g_i$ from the numerical model to follow (Sec. V), which uses a 10-eV occupied bandwidth with a 1-eV energy gap beginning at zero energy. The abrupt behavior shown at the bottom of the band deviates from the above-mentioned logarithmic behavior because near the bottom of a band the states are not perturbed weakly, and the above first-order perturbation relation for $S_{ij}$ becomes invalid. The rise at the top of the band marks the onset of the logarithmic divergence.

To obtain $h_n$ from Eq. (11), the term $g_i$ is summed with the inverse matrix element $s_{ni}^{-1}$ over occupied states $i$. Since the matrix $s$ is a submatrix of a unitary matrix in which elements only strongly couple states that are near in energy, we expect that $S_{in}^*$ should give an approximation to the value for $s_{ni}^{-1}$. Indeed, $S_{in}^*$ is the leading term for a series expansion

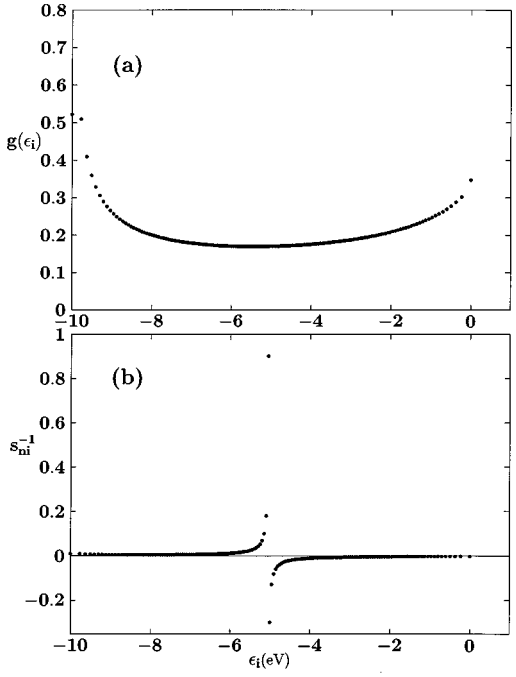


FIG. 1. An example of the behavior of $g(\epsilon_i)$ and $s^{-1}$ for the numerical model of Sec. IV, where $Nv=-2$ eV with a 1-eV band gap starting at $\epsilon_i=0$. In (a), $g_i$ is plotted vs $\epsilon_i$. In (b), $s_{ni}^{-1}$ is plotted vs $\epsilon_i$ for $n=80$ ($\epsilon_n=-5.049$ eV).

for $s_{ni}^{-1}$ developed in the Appendix. The leading term by itself is most accurate for the diagonal and near-diagonal elements, which are the most important terms when evaluating $h_n$, since these are the largest terms. The behavior of $s_{ni}^{-1}$ as a function of $i$ is then clear from the perturbation expression Eq. (15), for $S_{in}^*$. It consists of a single positive term with magnitude near 1 for $i=n$, otherwise the energy denominator decays with both positive and negative counterparts, similar to the numerically determined $s_{ni}^{-1}$ of Fig. 1(b). $S_{in}^*$ can always be chosen to be zero for states $n$ degenerate with state $i$.

With $S_{in}^*\approx s_{ni}^{-1}$, and if there are sufficient occupied terms above and below in energy from state $n$ in the sum over $i$ defining $h_n$, then we observe in the $i$ summation of the product $s_{ni}^{-1}g_i$ that $s_{ni}^{-1}$ has the approximate effect of a Kronecker delta $\delta_{ni}$ picking out just the one term belonging to state $n$. This is because the decaying energy denominator wings will cancel when $g_i$ exhibits the slow logarithmic variation with $\epsilon_i$. Then $h_n$ effectively reflects the behavior of $g_n$, which for much of the spectrum varies slowly with $\epsilon_n$.

As the state $n$ moves towards the bottom of the band it would appear that removing the positive wing of the first-order expression to $S_{in}^*\approx s_{ni}^{-1}$, together with the variation of $g_i$ there, would produce structure to $h_n$. This will not be the case, since the orthogonalizing effect of $s^{-1}$, leading to the final-state rule, must result for these states that are far in energy from unoccupied states. Here, as mentioned above, it is expected that $s_{ni}^{-1}\approx S_{in}^*$ deviates from the simple behavior for $S_{in}^*$ given by first-order perturbation theory, enough so as to prevent any rapid variation to $h_n$. On the other hand, as the state $n$ moves closer in energy toward unoccupied states, the negative wing of $s_{ni}^{-1}$ will start to be removed. Here, within the one-body problem for metals, the quantities $S_{ij}$ are not sensitive to where the occupation boundary is, and thus Eq. (15) is expected to hold. Also, at least for semiconductors, $s_{ni}^{-1}$ still does not deviate considerably from $S_{in}^*$, since a finite band gap tends to keep $s$ closer to a unitary matrix (see Appendix). Now, near the unoccupied states, the removal of the negative wing for $s_{ni}^{-1}$ further enhances the emerging logarithmic divergence of $g_n$. In metals, this sharp cutoff at the Fermi energy is critical for the transformation from the logarithmic behavior of $g_n$ to a power-law divergence. If the system is a metal without an energy gap, the Mahan asymptotic power law divergence for metals arises as unoccupied states are approached.

Using the previously discussed edge behavior for $g_i$, we check this assertion by examining $h_n$ near threshold ($\epsilon_n=0$). Summing the mixing term while maintaining the approximation $s_{ni}^{-1}\approx S_{in}^*$ gives

$$h_n=\sum_{i=\mathrm{occ}} s_{ni}^{-1}g_i\approx\sum_{i=\mathrm{occ}} S_{in}^*g_i \tag{16}$$

$$\approx z\sum_{i=\mathrm{occ}}\left(\delta_{in}g_i-\frac{|v|g_i}{\epsilon_i-\epsilon_n}\right). \tag{17}$$

Near threshold,

$$h_n\propto -zn_0|v|\ln|\epsilon_n|+(zn_0|v|)^2\mathrm{P}\int_A^0\frac{\ln|\epsilon_i|d\epsilon_i}{\epsilon_i-\epsilon_n}, \tag{18}$$

where P indicates the principal value, and $A$ is some lower integration limit. The diverging contributions[16] give

$$\Lambda_n\propto\rho^2\left|1+\ln|\epsilon_n|^{-zn_0|v|}+\tfrac{1}{2}(\ln|\epsilon_n|^{-zn_0|v|})^2\right|^2, \tag{19}$$

which is recognized to contain the first few terms in the series for $\exp(\ln|\epsilon_n|^{-zn_0|v|})$, as similarly done in Ref. 1, thus pointing to the power-law expression,

$$\Lambda_n\propto\rho^2|\epsilon_n|^{-z2n_0|v|}. \tag{20}$$

For the threshold behavior in a metal, $n_0$ should correspond to the density of states $n_F$ at the Fermi energy. Furthermore, $n_F|v|$ can be identified with $\delta_F/\pi$ in the Born approximation.

This analysis is of course not exact given the lower-order approximations, but it does lead beyond the logarithmic divergence, and to the power-law divergence for metals. Indeed, in their analysis to demonstrate the final-state rule, Von Barth and Grossman[8] treat a metal with a contact potential in an approximation that ignores shakeup, and thus equivalent[17] to the use of the partially inverted initial state. They obtain the power-law form of the Mahan edge singularity for the asymptotic limit of the edge region. Here we have instead developed and maintained a general discussion where Eq. (9) remains suited for the analysis of semiconductors, which of course includes band structure, and without further Fourier transformation of a many-body response function.

In summary, throughout most of the spectrum, away from the band edge, $h_n$ varies slowly with the energy, as Fig. 2(a) illustrates for the factor $\Lambda_n$. Thus, producing an approximately uniformly enhanced final-state spectrum, reflecting a final-state rule. The above discussion points out that if a

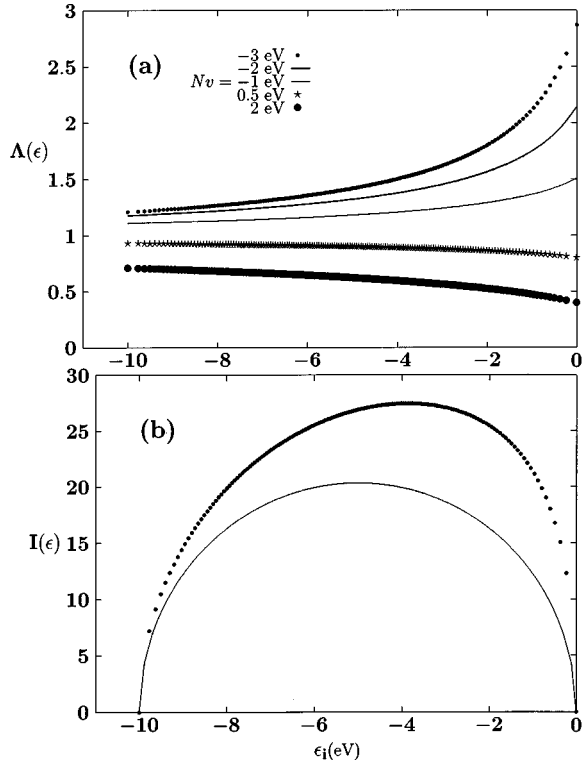


FIG. 2. The model calculation (a) for the factor $\Lambda$ is plotted vs the energy $\epsilon$ for several values of $v$ with $\epsilon_g = 1$ eV. For those instances where $Nv$ is positive, the specified value for $v$ represents the interband matrix element only, while $-2$ eV is used for the intraband matrix element. In (b) we show the corresponding emission (points) for the case $Nv = -2$ eV. The associated occupied density of states (solid) also gives the relative emission using the final-state rule.

small gap exists, the aborted divergence can still leave an enhanced band edge [Fig. 2(b)]. We will find that both the band-edge enhancement, and the approximate uniform enhancement, are not expected to be negligible.

## IV. ABSORPTION

Within the MND model, it has been demonstrated by Mahan[7] that absorption may be analyzed as the emission of holes from the unoccupied states. In such instance, the initial states for holes are the corresponding undistorted electron states, since the core-hole does not exist initially in the case of absorption. According to the prescription given here for emission, corresponding to Eq. (8), the appropriate partially inverted initial state $|\overline{\psi}_n\rangle$ to use in hole emission to describe electron absorption to the unoccupied state $n$ is then is given by

$$|\overline{\psi}_n\rangle = |\phi_n\rangle + \sum_{j=\mathrm{occ}} (\overline{s^\dagger})^{-1}_{ni} \sum_{i=\mathrm{unocc}} S^\dagger_{ij} |\phi_j\rangle$$

$$= |\phi_n\rangle + \sum_{j=\mathrm{occ}} (\overline{s^{-1}})^*_{in} \sum_{i=\mathrm{unocc}} S^*_{ji} |\phi_j\rangle, \qquad (21)$$

where $\overline{s}$ denotes the submatrix of $S$ corresponding to the *unoccupied* states only. Within the discussion of hole emission, one could define a matrix element $S'_{ji} = \langle \phi_i | \psi_j \rangle = S^*_{ji} = S^\dagger_{ji}$, in direct correspondence to the case of electron emission, but the unecessary definition is avoided with the adjoint operation.

For the MND problem, the initial formulation of Ohtaka and Tanabe[12] is based from the viewpoint of absorption. Later,[18] an accounting for emission is obtained. Here we have instead taken the opposite approach. The OT result for the primary emission[19] is easily seen to conform with Eq. (3). The connection for absorption is not so obvious, since here we have described absorption using the inverse of the unoccupied submatrix, whereas the corresponding OT effective single-particle state $|\psi^{\mathrm{OT}}_n\rangle$ used to calculate absorption is given by

$$|\psi^{\mathrm{OT}}_n\rangle = |\phi_n\rangle - \sum_{m=\mathrm{occ}} S_{nm} \sum_{j=\mathrm{occ}} s^{-1}_{mj} |\phi_j\rangle, \qquad (22)$$

which instead involves the inverse of the occupied submatrix.

The two relations Eq. (21) and Eq. (22) can be shown to be equivalent by using two identities[20] for partitioned matrices. For the matrix $A$, written in partitioned block form

$$A = \begin{pmatrix} A_{11} & A_{12} \\ A_{21} & A_{22} \end{pmatrix}, \qquad (23)$$

the identities are

$$[A_{22} - A_{21} A^{-1}_{11} A_{12}]^{-1} = (A^{-1})_{22}, \qquad (24)$$

and

$$[A_{21} A^{-1}_{11} A_{12} - A_{22}]^{-1} A_{21} A^{-1}_{11} = (A^{-1})_{21}. \qquad (25)$$

Here $(A^{-1})_{21}$ denotes the lower left block for the inverse of the *full* matrix $A$, whereas $A^{-1}_{11}$ denotes the inverse of the submatrix $A_{11}$

Upon partitioning the unitary matrix $S$ between occupied and unoccupied parts, the first identity implies

$$\left[ S_{in} - \sum_{k,p=\mathrm{occ}} S_{ik} s^{-1}_{kp} S_{pn} \right]^{-1} = S^\dagger_{in} = \overline{s^\dagger}_{in}, \qquad (26)$$

or

$$S_{in} - \sum_{k,p=\mathrm{occ}} S_{ik} s^{-1}_{kp} S_{pn} = (\overline{s^\dagger})^{-1}_{in} = (\overline{s^*})^{-1}_{ni}. \qquad (27)$$

Here, the indices $i$ and $n$ necessarily refer to unoccupied states, and $j$ refers to occupied states. With the second identity we have

$$\sum_{m=\mathrm{occ}, n=\mathrm{unocc}} \left[ \sum_{k,p=\mathrm{occ}} S_{ik} s^{-1}_{kp} S_{pn} - S_{in} \right]^{-1} S_{nm} s^{-1}_{mj} = S^\dagger_{ij} \qquad (28)$$

or

$$\sum_{m=\mathrm{occ}, n=\mathrm{unocc}} - S^*_{ni} S_{nm} s^{-1}_{mj} = S^*_{ji}, \qquad (29)$$

where $S^*_{ni}$ was substituted from the first identity. Multiplying both sides of Eq. (29) by $(\overline{s^*})^{-1}_{il}$ ($l$ unoccupied), then sum-

ming the index $i$ over unoccupied states and noting the resulting Kronecker delta, one obtains the desired connection

$$-\sum_{m=\mathrm{occ}} S_{nm} s^{-1}_{mj} = \sum_{i=\mathrm{unocc}} (\overline{s^*})^{-1}_{in} S^*_{ji}. \tag{30}$$

Substitution of this result into Eq. (21) demonstrates the equivalence of Eqs. (21) and (22).

Equation (9) for the primary emission is missing from the OT analysis. There,[5] it was lamented that the final-state rule for emission could not be clearly argued from their analytic results with the contact potential for a partially filled conduction band, because an analogous expression as for absorption, Eq. (22), was not available for the case of emission. We can obtain this counterpart relation by invoking a companion identity of Eq. (25), which is

$$A_{11} A^{-1}_{12} [A_{21} A^{-1}_{11} A_{12} - A_{22}]^{-1} = (A^{-1})_{21}. \tag{31}$$

In a similar procedure that lead to Eq. (30), this last identity yields

$$-\sum_{i=\mathrm{occ}} s^{-1}_{ni} S_{ij} = \sum_{m=\mathrm{unocc}} S^*_{mn} (\overline{s^*})^{-1}_{jm}. \tag{32}$$

Substitution of this relation into Eq. (8) gives

$$|\overline{\phi_n}\rangle = |\psi_n\rangle - \sum_{m=\mathrm{unocc}} S^*_{mn} \sum_{j=\mathrm{unocc}} (\overline{s^*})^{-1}_{jm} |\psi_j\rangle, \tag{33}$$

which is the missing analogous expression to absorption, Eq. (22), for the case of emission. We note that this is precisely what one would obtain using the OT absorption relation Eq. (22), but where one views emission as the absorption of holes. As far as recognizing which single-particle states are most suitable for a single-particle calculation, and obtaining an elementary understanding of the edge behavior, it seems here that an original viewpoint based on the emission process, Eqs. (3) or (8), rather than the absorption process, has been generally more illuminating for both the cases of emission and absorption, in semiconductors.

## V. A TWO-BAND MODEL

To address the question of whether the edge enhancement is significant in ordinary semiconductors, some reasonable estimates for the matrix elements $v_{ij}$ will be needed, as well as a model system to study. Previously,[5,21] numerical calculations within the MND model have often used a partially filled *single* band when modeling a metal. It is there observed that the emission spectra tend to exhibit quite different behavior dependent on the band filling. Such numerical calculations have indicated that the transition rate for a *completely* filled band reflects the final-state single-particle transition matrix elements, exactly, throughout the band. In light of Eq. (9), this is to be expected, since all unoccupied states have been exhausted, and thus the second term is zero. The other extreme is a band that is only slightly filled, and where initial-state single-particle transition matrix elements appeared appropriate.[22] In this case, we have that *all* occupied states are near in energy to unoccupied states. From the viewpoint taken here, one might be inclined to conclude that there are relatively few occupied components to orthogonalize with, leaving the distorted state essentially unaltered, thus suggesting an initial-state rule for the case of a slightly filled band. However, near the band minimum, the mixing between the two orthonormal sets due to the impurity potential is not as simple as the first-order perturbation relation would suggest. At least for the numerical model to be used here, the overlap elements $S_{ij}$ near the band minimum tend to have more weight toward states $j$ of lower energy from state $i$. Thus, orthogonalization to the few occupied states still may alter the initial distorted state significantly, yet the partial transformation is not complete enough to form a final state. Thus no part of the spectra need reflect the final-state or initial-state single-particle wave functions, and invoking an initial-state rule can be misleading. Therefore, no such conclusion is drawn here from the exact relations Eq. (3) or Eq. (8).

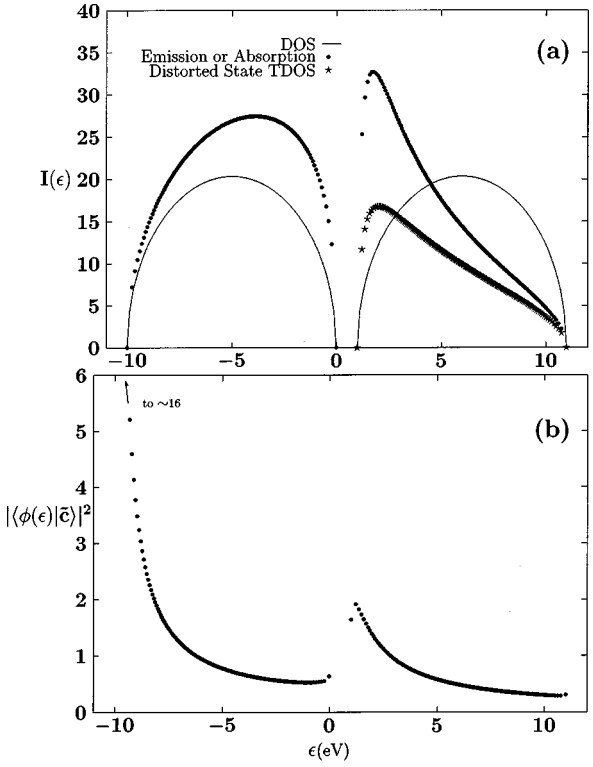


FIG. 3. Comparison (a) of the model emission and absorption for $Nv = -2$ eV. Also included is the TDOS for absorption, whereas here the TDOS for emission follows the DOS. In (b) we show the distorted state transition matrix elements $|\langle \phi(\epsilon)|\tilde{c}\rangle|^2$ consistent with $\langle \tilde{c}|\psi(\epsilon)\rangle = 1$.

In actual semiconductors, there are unoccupied states across a band gap. A two-band model is then appropriate, where one band is completely occupied. We employ two energy bands separated by a specified band gap [Fig. 3(a)]. Each band has an elliptical density of states (DOS) $n(\epsilon)$ given by

$$n(\epsilon) = \frac{2\sigma}{B}\left[\left(\frac{B}{2}\right)^2 - (\epsilon - \epsilon_0)^2\right]^{1/2}, \tag{34}$$

where $B$ is the bandwidth and $\epsilon_0$ is the center of the band. The parameter $\sigma$ controls the strength of the density of states and thus the total number of states. In the model calculation here, we use 161 states per band, which for a finite band gap

easily exceeded what is needed for satisfactory convergence of the spectral shape with regard to the level spacing. Given energies $\epsilon_i$ that conform to the modeled density of states, and appropriate matrix elements $v_{jk}$, the eigenvalue problem of Eq. (14) is solved numerically, yielding $S_{ij}$. The submatrix $s$ can then be numerically inverted, and the resulting spectra constructed.

The model parameters are chosen here with a semiconductor similar to silicon in mind, $B=10$ eV for each band, separated in energy by $\epsilon_g=1$ eV. As for the matrix elements $v_{ij}$ for the simple model here, we only desire to obtain some representative results using sensible numbers. For typical values of the matrix elements $v_{ij}$, we again rely on a negative constant quantity $v$, as done in the Koster-Slater[23] model. This is what tight-binding Bloch wave functions

$$\psi_i(\mathbf{r})=\sqrt{\frac{1}{N}}\sum_R \exp(\mathbf{k}_i\cdot\mathbf{R})\chi(\mathbf{r}-\mathbf{R}) \tag{35}$$

for $N$ lattice sites would have when the core-hole site is at the arbitrary origin, and the screened core potential is localized to the core-hole site. Here $\chi(\mathbf{r}-\mathbf{R})$ is a localized wave function about each lattice site $\mathbf{R}$, and $\mathbf{k}_i$ is the crystal momentum for state $i$.

To obtain a typical estimate for $v$, we employ self-consistent silicon $3s$ and $3p$ radial atomic wave functions[24] for $\chi(\mathbf{r}-\mathbf{R})$. One approach to the screening is to use a simple effective-mass impurity potential $-e^2/\kappa r$, where $\kappa$ is the static dielectric constant typical of a semiconductor. Another simple approach uses a Thomas-Fermi screening $(-e^2/r)\exp(r/\lambda)$ with screening length $\lambda$.

In the effective mass approximation using $\kappa=10$, whether evaluating matrix elements between $s$ states, $p$ states, or between $s$ and $p$ states, these atomic wave functions yield strengths for $v$ of $\sim$1.5 eV. For Fermi-Thomas screening with a screening length of 0.5 Å,[25] one obtains strengths of $\sim$3 eV or larger. We shall take the value of $Nv=-2$ eV as typical for all matrix elements.

We define the undistorted and distorted transition density of states (TDOS) with $n(\epsilon)|\langle\tilde{c}|\psi(\epsilon)\rangle|^2$ and $n(\epsilon)|\langle\phi(\epsilon)|\tilde{c}\rangle|^2$, respectively. Figure 2(a) shows the factor $\Lambda_n$ from the model calculation for several values of $v$. This factor is the enhancement factor that multiplies the undistorted final-state TDOS, which for this case where we choose $\langle\tilde{c}|\psi_n\rangle=1$, is identical to the modeled DOS. For $Nv=-2$ eV, we observe for $\Lambda_n$, a slow rise of 25% within the lower 70% of the band, then an additional 50% gain just within the remaining band-edge region with a range of 3 eV. Significant effects occur even for $Nv=-1$ eV. Diminishing the band gap, as well as narrower bandwidths, will increase the effect also.

Calculations for the emission spectra of silicon[26,27] have always lacked enough strength near the band-edge region when efforts are invoked to sensibly select the energy-dependent valence-hole lifetime broadening to help fit the calculation to the remaining experimental spectrum. This model calculation indicates that the band-edge modification can be significant even for semiconductors, and that band-structure calculations need to include the contributions of the second term of Eq. (9) in calculating emission and near-edge absorption spectra from single-particle self-consistent wave functions. Here we see that the missing emission strength near the band edge could very well be accounted for by this band-edge enhancement.

Even with a tight-binding model in mind, the interband matrix elements, as well as the intraband matrix elements from different bands, need not be the same constant. It is of course the matrix elements that couple between occupied and unoccupied states, which are most significant with regard to the spectral shape modifications discussed here. In semiconductors these will be interband matrix elements, in contrast to metals where the intraband matrix elements are most important. In a tight-bonding model the intraband matrix elements are necessarily negative for an attractive potential. However, the interband matrix elements need not be negative. This will depend critically on the screening distance, since this length will determine the range of integration in determining $v_{ij}$. If the interband elements were to be predominantly positive, the band-edge enhancement instead becomes a suppression [Fig. 2(a)] of the band edge.

A modified screening may be an important effect in the interpretation of data for x-ray resonant inelastic scattering,[28,29] since both the ordinary emission process discussed here, and the resonant scattering occur with comparable contributions. The x-ray resonant scattering is a single coherent absorption and emission process, unlike the ordinary incoherent two-step process that has been addressed here. The resonant scattering typically occurs for photon energies that would promote the core electron to a localized core exciton state. Such a final state will produce a different screening than that obtained by self-consistent delocalized states. The formalism described here shows that a modified screening can strongly alter the emission spectra. Whether the modified screening suppresses or enhances the edge region, it would be important to the analysis of the resonant inelastic scattering to understand any modifications for the subtraction of the incoherent contribution.

Although band structure plays a lesser role in absorption well above threshold, as recognized in the theory of extended x-ray absorption fine structure (EXAFS), near threshold where the photoelectron mean free path is relatively large, the two-band model calculation is still relevant. Results from the model calculation for $Nv=-2$ eV for both emission and absorption, are also shown in Fig. 3. For the model calculation of absorption, using the effective single-particle states defined with Eq. (21), the matrix elements $\langle\phi_n|\tilde{c}\rangle$ should be consistent with the choice $\langle\tilde{c}|\psi_n\rangle=1$. Hence

$$\langle\phi_n|\tilde{c}\rangle=\sum_{k=\text{all}} S^*_{nk}\langle\psi_k|\tilde{c}\rangle=\sum_{k=\text{all}} S^*_{nk}. \tag{36}$$

Thus here, for absorption, the distorted state TDOS is different in Fig. 3(a) from both the DOS and the exactly calculated absorption. The threshold enhancement for absorption at the band edge, beyond the final-state distorted TDOS, is evident. Furthermore, since in semiconductors the shakeup is absent at the edge region, there exists a clear distinction between the edge enhancement in absorption due to the final-state interactions, and the many-particle dynamic exchange enhancement. For both emission and absorption, the model calculation predicts large effects beyond the final-state TDOS, particularly with regard to the absolute transition rates. Ex-

perimental data rarely measure absolute rates, therefore it is the spectral shapes near the band edges that will ordinarily reveal the band-edge modifications described here. If the exact absorption is normalized to the same area as the distorted TDOS of absorption, the model calculation with $Nv=-2$ eV still shows a ~25% threshold enhancement due to the dynamic exchange effect.

Figure 3(b) shows the matrix elements $|\langle\phi(\epsilon)|\tilde{c}\rangle|^2$ consistent with the choice $\langle\tilde{c}|\psi_n\rangle=1$. The figure aides in the appreciation of the final-state rule in emission, while Fig. 2(a) indicates to what extent the uniform enhancement (or suppression) factor relevant to the final-state rule is constant over most of the band.

## VI. SUMMARY AND CONCLUSION

In emphasizing that the Anderson orthogonality is not expected to occur for filled band materials, we have discussed, for semiconductors, a simple and rather complete description within the MND model of x-ray spectra from electronic transitions alone. The shakeup contribution is not at all critical within the x-ray edge regions, and can then be addressed as a distinct smaller effect further away from the edge regions in both emission and absorption. The many-particle modification from the final-state TDOS in the core spectra of semiconductors is described within a formalism, embodied in Eq. (9), which is based on single-particle wave functions and the impurity scattering problem. The formalism is thus practical for materials with band structure, and not restricted to the model scattering matrix elements used here. The present model calculation has illustrated these spectral modifications in a simple two-band picture, and demonstrates that these effects can be significant, thus indicating that any realistic calculation of emission or absorption for a filled band material with a relatively small band gap should include the mixing term contribution of Eq. (9). A treatment for the case of silicon is currently in progress. We have also clarified the connection for absorption to the determinantal technique of Ohtaka and Tanabe with the approach used here.

For semiconductors, a calculation that yields good self-consistent wave functions for both occupied and unoccupied states, using matrix elements modified according to Eq. (9), would be expected to obtain better agreement with emission spectral shapes in the band-edge region. If realistic calculations indeed obtain good agreement in the band-edge regions, the formalism should be particularly important in experimental analysis for the scaling of data to theoretical calculations, since near the edge regions in semiconductors, unknown factors from other physical processes such as the valence-hole lifetime broadening and shakeup are absent or minimized. A confident scaling using this region of data can begin to distinguish and clarify these other many-particle contributions to core x-ray spectra that occur in other spectral regions. Hence, further many-body effects can be experimentally investigated. The formalism also makes a clear distinction between an exitonic versus a many-particle dynamic exchange enhancement in absorption edges of filled band materials. Finally, the effective single-particle state used here should also be relevant to the calculation of near-edge x-ray absorption fine structure.

## APPENDIX

It is of analytic interest to have a series expansion for $s^{-1}$. The unitary condition

$$\sum_{n=\mathrm{occ}} S_{in}^* S_{kn} + \sum_{n=\mathrm{unocc}} S_{in}^* S_{kn} = \delta_{ik} \tag{A1}$$

may be written, for $k$ and $i$ occupied, as

$$\sum_{n=\mathrm{occ}} S_{in}^* S_{kn} = \sum_{j=\mathrm{occ}} s_{ij}^* (s^*)_{jk}^{-1} - \sum_{n=\mathrm{unocc}} S_{in}^* S_{kn} . \tag{A2}$$

Multiplying by $(s^*)_{pi}^{-1}$, with $p$ occupied, and summing over occupied states $i$ gives

$$\sum_{n=\mathrm{occ}} S_{kn} \sum_{i=\mathrm{occ}} (s^*)_{pi}^{-1} S_{in}^* = \sum_{j=\mathrm{occ}} (s^*)_{jk}^{-1} \sum_{i=\mathrm{occ}} (s^*)_{pi}^{-1} S_{ij}^* - \sum_{i=\mathrm{occ}} (s^*)_{pi}^{-1} \sum_{n=\mathrm{unocc}} S_{in}^* S_{kn} , \tag{A3}$$

or

$$\sum_{n=\mathrm{occ}} S_{kn} \delta_{pn} = \sum_{j=\mathrm{occ}} (s^*)_{jk}^{-1} \delta_{pj} - \sum_{i=\mathrm{occ}} (s^*)_{pi}^{-1} \sum_{n=\mathrm{unocc}} S_{in}^* S_{kn} , \tag{A4}$$

and hence

$$s_{kp}^{-1} = S_{pk}^* + \sum_{i=\mathrm{occ}} s_{pi}^{-1} \sum_{n=\mathrm{unocc}} S_{in} S_{kn}^* . \tag{A5}$$

By defining the matrix $f_{ik}=\Sigma_{n=\mathrm{unocc}} S_{in} S_{kn}^*$, and retiterating Eq. (A5), one obtains the series expansion

$$s_{pj}^{-1} = S_{jp}^* + (fs)_{jp}^* + (f^2 s)_{jp}^* + (f^3 s)_{jp}^* + \cdots . \tag{A6}$$

In comparing to the model calculations used here, the series convergence properties will depend on the ratio of $Nv$ to the band gap. For numerical calculations with $Nv=-2$ eV and a 1-eV band gap, all elements converge rapidly, particularly the diagonal and near-diagonal elements. Convergence is poorest for elements that are the least diagonal elements that also are next to the energy boundary with unoccupied states. With only the second series term included, the percentage deviation from the exact inverse was found to be 1% for the poorest converging terms, and two orders of magnitude better for the diagonal terms. As might be expected, when the energy gap closes, as for a metal, convergence becomes less rapid. Nevertheless, for energy gaps equal to the energy level spacing, and $Nv=-2$ eV, numerical examination for larger and larger systems, with smaller level spacing, indicates that the two-term truncated series sum remains accurate to 1% for the diagonal inverse matrix elements. Furthermore, inclusion of the third term gives at least 10% accuracy for the least convergent inverse matrix elements.

[1] G. D. Mahan, Phys. Rev. **153**, 882 (1967).
[2] P. Nozières and C. T. DeDominicis, Phys. Rev. **178**, 1097 (1969).
[3] P. W. Anderson, Phys. Rev. Lett. **18**, 1049 (1967).
[4] G. D. Mahan, in *Solid State Physics*, edited by H. Ehrenreich, F. Seitz, and D. Turnbull (Academic, New York, 1975), Vol. 29, p. 771.
[5] K. Ohtaka and Y. Tanabe, Rev. Mod. Phys. **62**, 929 (1990).
[6] U. von Barth and G. Grossman, Solid State Commun. **32**, 645 (1979).
[7] G. D. Mahan, Phys. Rev. B **21**, 1421 (1980).
[8] U. von Barth and G. Grossman, Phys. Rev. B **25**, 5150 (1982).
[9] U. von Barth and G. Grossman, Phys. Scr. **28**, 107 (1983).
[10] J. Friedel, Comments Solid State Phys. **2**, 21 (1969).
[11] M. Combescott and P. Nozières, J. Phys. (Paris) **32**, 913 (1971).
[12] K. Ohtaka and Y. Tanabe, Phys. Rev. B **28**, 6833 (1983).
[13] P. Livins and S. E. Schnatterly, Phys. Rev. B **37**, 6731 (1988).
[14] L. C. Davis and L. A. Feldkamp, Phys. Rev. B **23**, 4269 (1981).
[15] T. A. Green, Phys. Rev. B **32**, 3442 (1985).
[16] Indefinite integrals for the evaluation of the principal value are found in A. P. Prudnikov, Yu. A. Brychkov, and O. I. Morichev, in *Integrals and Series* (Gordon and Breach Science, New York, 1986), p. 244.
[17] Combine Eqs. (6.7) with Eq. (6.2) of Ref. 8.
[18] T. Kita, K. Ohtaka, and Y. Tanabe, J. Phys. Soc. Jpn. **56**, 4609 (1987).
[19] Equation (4.53) of Ref. 5, for instance.
[20] R. A. Horn and C. R. Johnson, *Matrix Analysis* (Cambridge University Press, New York, 1985), p. 18.
[21] V. I. Grebennikov, Y. A. Babanov, and O. B. Sokolov, Phys. Status Solidi B **79**, 423 (1977).
[22] J. W. Wilkins, in *X-ray and Atomic Inner-Shell Physics*, AIP Conference Proceedings No. 94, edited by B. Craseman (AIP, New York, 1982), p. 687.
[23] G. F. Koster and J. C. Slater, Phys. Rev. **95**, 1167 (1954).
[24] F. Herman and S. Skillman, *Atomic Structure Calculations* (Prentice-Hall, Englewood Cliffs, NJ, 1963).
[25] K. W. Boer, *Survey of Semiconductor Physics* (Van Nostrand Reinhhold, New York, 1990), p. 361.
[26] J. Klima, J. Phys. C **3**, 70 (1970).
[27] R. D. Carson, Ph.D. dissertation, University of Virginia, 1989.
[28] K. E. Miyano, D. L. Ederer, T. A. Callcott, W. L. O'Brien, J. J. Jia, L. Zhou, Q.-Y. Dong, Y. Ma, J. C. Woicik, and D. R. Mueller, Phys. Rev. B **48**, 1918 (1993).
[29] Y. Ma, P. Skytt, N. Wassdahl, D. C. Mancini, J. Guo, and J. Nordgren, Phys. Rev. Lett. **71**, 3725 (1993).